

Antibacterial and anti-quorum sensing activity of Poly(amidoamine) Generation 4 loaded Quorum Quencher peptide against MRSA, *Staphylococcus aureus* and *agr* mutants

Naifa A. Alenazi^{1*}, Fadilah S. Aleanizy¹, Fulwah Y. Alqahtani¹, Abdullah A. Aldossari², Mohammed M. Alanazi², Rihaf T Alfaraj¹

¹Department of Pharmaceutics, College of Pharmacy, King Saud University, Riyadh 11495, Saudi Arabia

²Department of Pharmacology and Toxicology, College of Pharmacy, King Saud University, Riyadh 11495, Saudi Arabia

ABSTRACT: Methicillin-resistant *Staphylococcus aureus* (MRSA) is the predominant pathogen responsible for antimicrobial resistance in both community and healthcare settings. A promising approach to combat MRSA is to target its quorum sensing (QS) system. The objective of this study was to target the QS in MRSA using a novel quorum quencher (QQ) peptide called QQ3, which acts as a histidine kinase inhibitor. However, therapeutic peptides have limitations, such as poor membrane permeability and insufficient in vivo stability. To address these limitations, this investigation used PAMAM dendrimers generation-4 (G4) as a nanocarrier for the peptide, as they possess antimicrobial properties, to enhance stability, facilitate efficient drug delivery, and increase potency. The average particle size of the formulated G4-QQ3 complex was determined to be 268nm, with a polydispersity index value of 0.32. The minimum inhibitory concentration (MIC₅₀) for the formulated nanoparticles was found to be 20μM, as demonstrated by a growth assay. Additionally, the hemolysis activity of MRSA was inhibited at a concentration of 10μM. The G4-QQ3 complex exhibited the ability to inhibit, penetrate, and eradicate biofilm in MRSA strains, with inhibition percentages ranging from 63 to 70%. Furthermore, the cytotoxicity of the formulation against RAW 264.7 cells indicated that the nanoparticles were cytocompatible. This study confirms that encapsulating the QQ3 peptide within PAMAM G4 dendrimers results in a potent anti-virulence and antibacterial effect. These findings have significant implications for the development of novel treatments for MRSA infections.

INTRODUCTION

MRSA refers to methicillin-resistant *Staphylococcus aureus*, a bacterium resistant to many available antibiotics, including β-lactam. MRSA is the predominant pathogen contributing to antimicrobial resistance (AMR) in both community and health care settings. *S.aureus* is an opportunistic pathogen that can cause serious infections and are difficult to treat. This resistance strains are responsible for many serious infections, including device-related infection, osteomyelitis, endocarditis, urinary tract infection, and skin soft tissue infections; those infections are associated with high morbidity and mortality compared to other organism¹. MRSA is the main cause of infections than multi-drug resistant (MDR) pathogens combined. Also, depending on the World Health Organization (WHO), MRSA is classified as one of the 12 priority pathogens that threaten human health. In Saudi Arabia the prevalence rate of MRSA is 38% and it considered the highest between gulf countries. The rate of MRSA prevalence in the Western 42%, Central 32%, and Eastern region was 27% [1].

The consequences of MRSA infection continue to increase, and the reasons for this increase includes the increases in transmission rates, intense colonization, and rapid bacterial activation of virulence factors that increase the infection's pathogenicity [2]. Overuse of antibiotics has been associated with resistance in hospitals and communities. The antibiotic resistance is a serious and growing global threat that may herald the end of the antibiotic era. Resistance makes some of these antibiotics entirely ineffective, and it occurs incidentally by gene mutation or acquisition of the resistance gene from other bacteria by plasmid transfer [2]. Quorum sensing (QS), is a mechanism which allow a cell-to-cell communication due to population expanding of the bacteria. In MRSA quorum-sensing accessory gene regulator (*agr*) system control the virulence factors production. Therefore, at high cell density *agr* is activated lead to secret an autoinducing peptide (AIP). These AIP are detected by the transmembrane receptor leading to activate the virulence factors to enhance the ability of the bacteria to cause infection. During invasion, *agr* is activated, and colonisation with MRSA has been associated with downregulation of *agr* system and diminished expression of toxins, but increased biofilm formation. Also, it has been reported that activation of the *agr* system is necessary for detachment of biofilm. So, *agr* system is necessary for established and detachment of biofilm, it regulates the switch between planktonic and biofilm lifestyles [3]. For biofilm established AIP is required that may activate the *agr* system, and for detachment extracellular proteases activity is needed, and the target of these *agr* controlled genes is not clear. The biofilm formed by *agr* mutants are thicker and smother than WT [4].

MRSA pathogenicity is highly dependent on the virulence factors such as toxins (Hemolysins), immune-evasive surface factors (capsule and protein A), and biofilm formation [3]. MRSA has two QS system produced by *agr* locus; RNAPII originate from the P2 promoter, and RNAPIII originate from P3 promoter. The RNAPIII segment of *agr* is generated from four genes *agrBDCA*, which encode all the main components of QS system. The transmembrane protein *agrB* involve in; AIP secretion, and *agrD* processing. Whereas, the *agrA* encodes the cytosolic response regulator (RR), and *agrC* encodes membrane-bound histidine kinase (HK) and both forms the two-component regulatory system (*AgrAC* TCS) [5]. TCS are tools to regulate the interaction, adaption to condition, and survival in the human host environment. TCSs are highly conserved domine and the main signal transduction pathways the bacteria used to regulate many processes including metabolism, virulence, protein interaction, and antibiotic resistance [6]. The *AgrC* receptor-histidine protein kinase binds to AIPs and upon binding leads to phosphorylates of *AgrA* in the cytosol. Then it will bind to P2 and P3 leads to stimulate the transcription of regulatory RNA-II, RNA-III, and expression of virulence factors. Therefore, the two-component system is important for bacterial life and death and is required for resistance to common antibiotics. This makes these components a promising target for discovering novel antibacterial activity. The inhibition of autophosphorylation of HK will result in a broad-spectrum antibacterial activity. Also, the folding of the CA domine in the HK in bacterial cell is different from the folding in the mammalian cell, this gives a selectivity for the inhibitor with reduces side effects [7]. Increasing antibiotic resistance and diminishing the development of new antibiotics by the pharmaceutical industry represent a global crisis that creates a need for alternative anti-infective strategies. These resistance strain can cause serious infections that are difficult to treat, with limited medication options available. One of the new strategies for facing these resistance pathogens is by targeting the virulence factor in the bacteria.

A novel macrocyclic peptide was discovered by Random non-standard Peptide Integrated Discovery (RaPID) system. This peptide was potent *agr* quorum quenchers and reduced the virulence factors in *S.aureus* by competitive binding to the sensor histidine kinase *AgrC* and inhibiting its function [8].

In agreement with previous studies [9,10]. HK of the TCS is an attractive target for antibacterial and anti-quorum sensing agents. Targeting a virulence such as QS is a new strategy that will reduce the evolution of bacteria to develop resistance. Because it disrupts the upstream regulatory functions of the bacterial physiology that leads to suppressing a series of virulence factors. While, conventional antibiotics targets only a specific bacterial protein that will impair the downstream functions. Combining conventional antibiotic with drug targeting this system will result in an effective antimicrobial agent and the potential to develop resistance will be minimum [11].

With their unique structure, dendrimers are considering a promising drug delivery system with reduced cytotoxicity. It is highly ordered branched macromolecules with well-defined, homogeneous 3-dimensional structures. Poly-amido-amine (PAMAM) dendrimers have accessible interiors that can be used to encapsulate molecules. They have antimicrobial properties, and high drug loading capacity [13].

Anionic and amphiphilic dendrimers can escape from the immune cell and provide target delivery for the infected cell. PAMAM-dendrimers conjugated with a membrane-interacting peptide were found to be active against herpes simplex virus and inhibit the virus replication. Another study used dendrimer antimicrobial peptides named G3KL was tested against multidrug resistance *P.aeruginosa* clinical isolates. The results demonstrates that induction of spontaneously resistant mutants with the dendrimer was difficult due to the fast-killing effect of the dendrimer [14].

Treating MRSA infection is a huge challenge; this investigation applied a new strategy for treating MRSA strains with a new anti-virulence agent using nanotechnology. The study targeted the QS-system in MRSA by using a new QQ peptide (QQ3 figure 1) that considers a potential HKI of the TCS. The peptides are subject to two inherent limitations, namely, membrane impermeability and inadequate in vivo stability, which pose significant challenges to the development of peptide-based drugs. The study used PAMAM generation 4 (G4) (1,4-diaminobutane core, carbomethoxypyrrolidone-terminated) dendrimers with antimicrobial properties to encapsulate the QQ3-peptide for efficient drug delivery, enhanced stability, and augment potency. The study confirms that encapsulating QQ3 peptide within PAMAM G4 dendrimer results in a potent anti-virulence and anti-bacterial action and suggests a synergism effect.

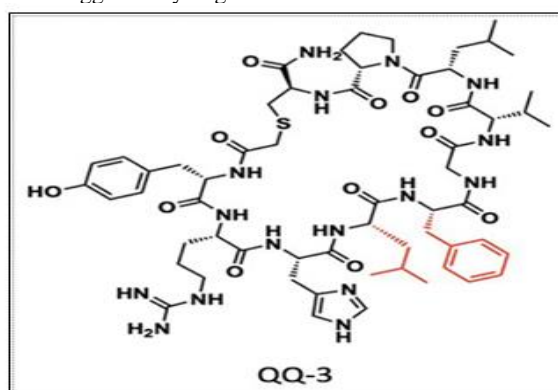


Figure 1. One of the new quorum quencher (QQ) peptide QQ3 [1].

MATERIALS AND METHODS

2.1. Materials

Zetasizer Nano ZS90 (Malvern Instruments Ltd, UK) will be used to measure the zeta potential, polydispersity index (PDI), and particle size of the formed nanoparticles. Transmission electron microscopy (TEM) (JEM1230EX; Tokyo, Japan); QQ3 was obtained from Pepmic Co., Ltd (China), cells were obtained from Sigma Aldrich (St. Louis, MO, USA). Polyamidoamine dendrimer generation 5 (PAMAM dendrimers G4, 1 g vial) was purchased from Nanosynthons (Mt. Pleasant, MI, USA), RAW 264.7 a macrophage cell proliferation kit I (MTT) was provided from American Type Culture Collection (ATCC). Bacterial strains wild type and mutants will be obtained from the library of MRSA transposon from the University of Washington Genome Centre (Washington University, Washington, Seattle, USA).

2.2. Bacterial strains and growth condition:

All bacterial strains listed in table 1 were grown at 37°C for 18-24 hr in Tryptic Soy Broth (TSB) and Tryptic Soy Agar (TSA) supplemented with erythromycin 15 µg/mL as a selective marker.

Table 1. Strains used in this study.

Strain name	Abbreviation	Description
<i>Staphylococcus aureus</i>	SA	Wild type
Methicillin-resistance <i>Staphylococcus aureus</i>	MRSA (ATC32200)	Methicillin resistance <i>Staphylococcus aureus</i> (use as control in Saudi Arabia hospital)
Accessory gene regulator A	$\Delta agrA$ gene	NE1532 4 P16 <i>agrA</i> accessory gene regulator protein A SAUSA300_1992
Accessory gene regulator C	$\Delta agrC$ gene	NE873 B17 <i>agrC</i> accessory gene regulator protein C SAUSA300_1991

2.3. Formulation of G4-QQ3 complex:

Loading the QQ3 into the PAMAM dendrimer was achieved using molar ratio of 1:1 for each. 1g of G4 PAMAM dendrimers was dissolved into 10 ml of Milli-Q water to give a concentration of (10% w/v) and QQ3, 24 mg dissolve in 10 ml Milli-Q water given a concentration of 2.4mg/ml. Then The amounts of G4 PAMAM dendrimers and QQ3 were calculated and added to the reaction mixture, with continuous stirred for 24 hours in the dark at 4 °C. then the complex was stored at (– 30) for further use.

2.4. Characterization of G4 complex:

The vesicles size and polydispersity index (PDI) were determined for the complex and blank PAMAM dendrimer G4, using the Zeta sizer Nano ZS (Malvern Instruments, UK). Dilution 1:5 ratio in Milli-Q water for the formulation was used and the zeta potential was also measured by Zeta sizer Nano ZS (Malvern Instruments, UK).

2.5. Transmission Electron Microscopy (TEM)

The blank of PAMAM dendrimer G4 and G5 and their complexes were visualized using Transmission Electron Microscopy (TEM) in order to evaluate the size and morphology.

2.6. Determination of drug encapsulation efficiency (EE%):

In-direct method was carried out using dialysis membrane. The G4-QQ3 complexes was placed into a cellulose membrane with MWCO 12000 Da, then immersed in deionized water and stirred for 1 hour at 4 °C. After that, 1 ml of from the media was withdrawn and analysis by HPLC. EE% was calculated by the following equation:

$$\% \text{Entrapment Efficiency} = \frac{\text{total amount of drug loaded} - \text{free drug in supernatant}}{\text{total amount of drug loaded}} \times 100 \quad (32)$$

Instrumentation and Chromatographic Conditions

The analysis of the QQ3 peptide was performed at Jazeera Pharmaceutical Industries Ltd. (Riyadh, Saudi Arabia). The method for analysis was conducted according to the company reference sheet for analysis of the QQ3 peptide. The separation was carried out at 25°C, using column Luna 5U (C18, 150x4.6, 3 µm) and the mobile phase was a linear gradient of a mixture of water and acetonitrile, both containing 0.1% (v/v) TFA, at a flow rate of 0.5 mL/min, the injection volume was 20 µL, wavelength 214 nm and the run time was 10 min. The mobile phase solutions were degassed using a sonicator and filtered through a 0.45 µm filter and the software utilized for data analysis was Agilent ChemStation.

In vitro release of the QQ3-G4 complex:

Briefly; About 200 µL of G4-QQ3 complex were taken in a dialysis cellulose membrane with a molecular weight MWCO12000Da. The dialysis bag was then immersed into beaker containing 20 mL of phosphate buffer saline (pH 7.4). The beaker was continuously shaken in a thermostat (37C). Around 500 µL of each sample was collected at specific time points for 4 days, and replaced every time with phosphate buffer saline. The samples were analyzed by HPLC, the percent of drug released was calculated at each time interval and plotted against time. The methods were conducted in triplicate.

Determination of minimum inhibitory concentration (MIC) on bacterial growth:

The concentrations of G4-QQ3 complex, and blank G4 that was able to inhibit the growth of 50 % of bacterial strains was determined using the bioscreen C system. Overnight culture of all bacterial strains was adjusted to an OD 0.08-0.1, then 200

µl of bacterial broth was added to 96 well plates. The plates were placed in Bioscreen C reader and the optical density of bacterial growth was recorded for 24 hr at wavelength 600 nm.

Biofilm inhibition assay:

Crystal violet assay (CV) staining was used to assess the effect of the MIC50% of the formulated nanoparticles and blank G4 against all bacterial strain's biofilm formation. Overnight culture was adjusted to an OD₆₀₀- 0.08-0.1, then 100 µl of bacterial broth suspension was inoculated in 96-well microtiter sterile plate, containing 100 µl of G4-QQ3 complex. The plate was incubated at 37 °C with continuous shaking at 150 rpm overnight. Planktonic cells were removed and the wells were washed twice time with of 0.9% NaCl and inverted to dry at room temperature for 1 h, then 0.1 % (v/v) crystal violet was added to the wells for bacterial staining for 15 min. Excess stain was removed and washed 3 times with 0.9 % NaCl, ethanol-acetone (80:20 v/v) was added to solubilized bound crystal violet. Absorbance of stained bacteria was measured by Elisa Plate reader.

Hemolytic Activity Analysis

Overnight cultures of bacterial strains were diluted to an OD 600-0.08–0.1, then small amount of the broth suspension was mixed with G4-QQ3 complex, and blank, G4 and spotted on to blood agar and incubated overnight at 37°C for 18h then at 4°C for 18 h. The hemolytic activity was observed on plates as transparency around the colonies.

Confocal Microscopy

Overnight culture of all bacterial strains was treated with MIC50% of the G4-QQ3 complex and with the blank G4. The effect of formulated nanoparticles on bacterial cell viability was investigated by confocal laser scanning microscope, with a Live/Dead® BacLight™ viability kit contain a universal stain SYTO 9 and propidium iodide (PI). Cells images were acquired using the Leica Application Suite Advanced Fluorescence software, with magnification power of 40× using an oil-immersion objective lens. An argon-based laser was applied for excitation at 488 nm, and HeNe laser for excitation at 543 nm. The SYTO 9 and PI emission was set at 528 nm and 645 nm respectively. by sequential scanning, the images were obtained and processed in Image J software.

Scanning Electron Microscopy (SEM)

To visualize biofilm formation, all bacterial strains were grown overnight in TSB at 37 °C. Then the cultures were adjusted to OD 600-0.08–0.1. Then Polyvinyl (Fisher Scientific) coverslips were placed in each well of a Thomas 6-well plate before being filled with 2 ml of TSB medium and 2 ml of diluted culture. Biofilms were formed on the coverslips at 37 °C for 24 hr. The samples were fixed with 3% glutaraldehyde in phosphate buffer pH 7.2 for 24 h, and washed 3 times, the samples were postfixed for 1 h with 1% osmium tetroxide (in H₂O). Then applied in to an ethanol dehydration series of 50, 60, 70, 80, 90, and 2 × 100% (v/v) ethanol, for 5 min at each concentration. The samples were dried for 1 day and sputter-coated with a palladium-gold film. The produced biofilm was viewed with a SEM/EDS system in a high-vacuum mode at 20 kV [16].

Cytotoxicity MTT Assay:

Macrophage RAW 264.7 cells were cultured in DMEM media with 10% fetal bovine serum, 1% penicillin, and 1% streptomycin and incubated with 5% carbon dioxide at 37°C. RAW 264.7 (5 × 10³ cells/well) cells were cultured overnight in 96-well plates and different concentrations (3 µM to 40 µM) of loaded nanoparticles and blank were added. The plates were allowed to continue incubation for 48 h. Finally, the cell viability was determined by kit I (MTT) assay. Absorbance at 570 nm was documented by micro-plate reader.

RESULTS

3.1. Characterization of Nanoparticles:

3.1.1. Particles size and ζ-potential

The result obtained from the Zetasizer showed the particle size of the blank G4 was 153 nm and when loaded with the QQ3 peptide the particle size was increased to 275.6 nm, less than 500 nm which considered in the nanosized range. The PDI value indicate no dramatic change between the loaded PDI= 0.32 and blank dendrimer PDI= 0.22, (p>0.05). The ζ-potential measurements for the blank G4 were -1.3 mV and it acquired the negative charge after loading to reach -19 mV due to the QQ3 negative charge, as demonstrated table 1.

Table 1. The particles size, PDI and ζ-potential.

Average	G4-QQ3 Complex	G4
Z average diameter (nm)± SD	268nm ± 10.1	158.2nm ± 8.2
Polydispersity Index (PDI) ± SD	0.32 ± 0.008	0.22 ± 0.005
Zeta potential (Mv) ± SD	-19 mV ± 0.57	-1.3 mV ± 1.07

3.1.2. TEM Images of G4-QQ3 complex and blank G4 treated bacterial biofilms:

The nanoparticles of G4-QQ3 complex, and blank G4 were observed with TEM (Figure 2) to have an almost spherical shape, especially in the blank nanoparticles, and a size of approximately 283nm and for the loaded nanoparticles G4-QQ3 complex, and blank G4 153nm. The difference in size between the blank and loaded nanoparticles proves that the loading of the drug was successful.

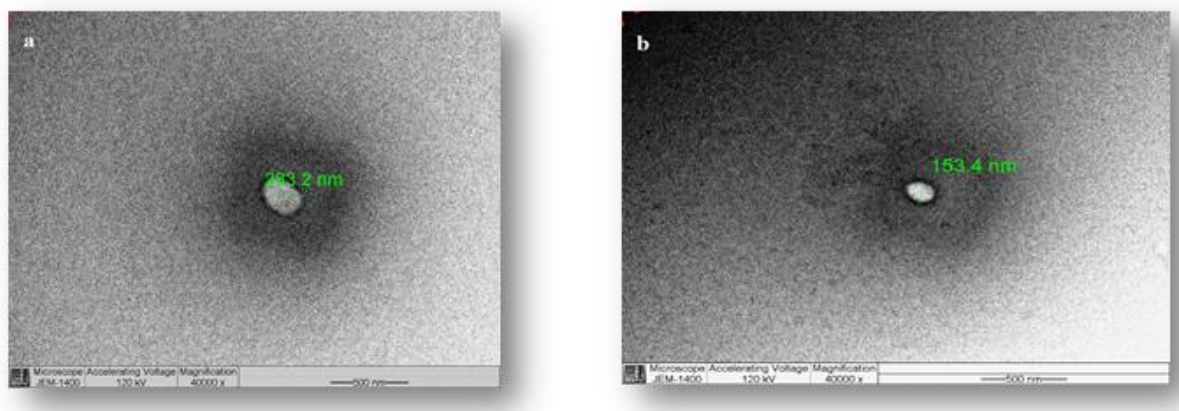


Figure 2. TEM images: (a) G4 loaded with QQ3 and; (b) Blank G4

3.2. Encapsulation efficacy.

The quantitative analysis of the G4-QQ3 complex to determine the encapsulation efficacy (EE%) was obtained from HPLC-UV showed a high percent of encapsulation efficiency equal to 98%.

3.3. In vitro Drug Release

In-vitro release of G4-QQ3 complex in 30 ml PBS buffer of pH 7.4 at $37 \pm 0.5^\circ\text{C}$, over 72 h as a time function was conducted using a dialysis membrane. The release profile of the loaded nanoparticles is plotted in figure 3, and it was characterized by a sustained flow manner and the percentage release of the peptide from dendrimer over 10 h was approximately 40 %. Then, the peptide release was gradually increased to reach 80% within 72 h.

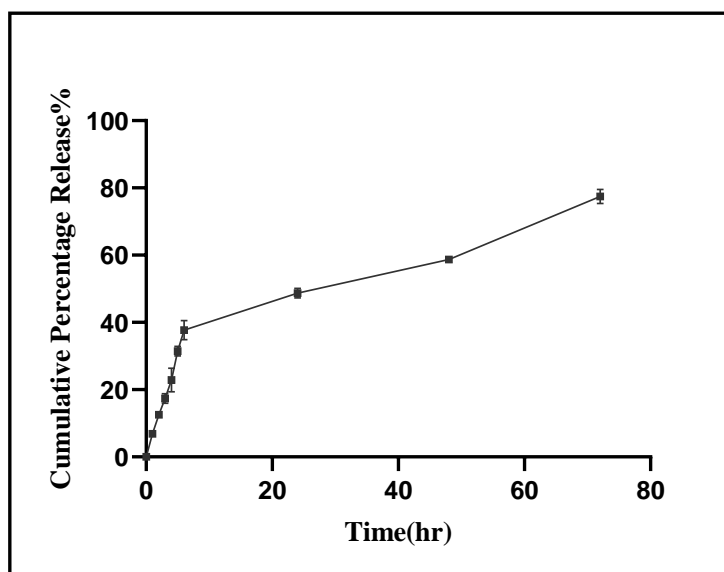
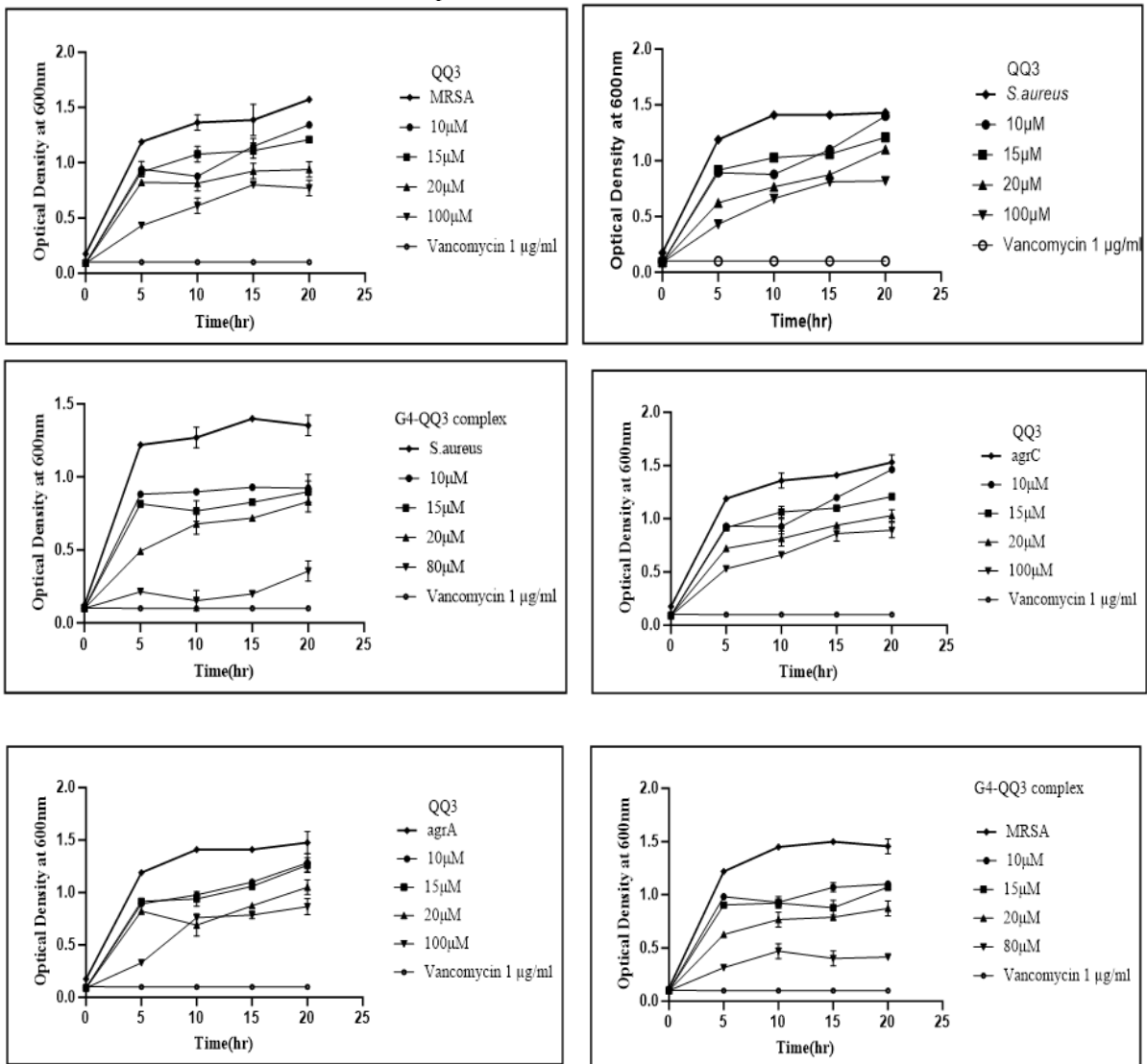


Figure 3. In-vitro release profile of QQ3-G4 comple. (mean \pm SD, n=3) ($p < 0.003$).

3.4. The Minimum Inhibitory Concentration (MIC) on bacterial growth:

G4-QQ3 complex and blank G4 were tested against all bacterial strains and Vancomycin was used as a positive control. The selected concentrations of the nanoparticles were range from $3\mu\text{M}$ to $100\mu\text{M}$ as showing in Figure 4. By adding the G4-QQ3 complex the growth of all strains was reduced as the concentration increased and the MIC₅₀ was determined based on the inhibition of the growth of 50 % of MRSA, *S.aureus*, *agrA*, and *agrC* population. The minimum inhibitory concentration (MIC₅₀) of the naked QQ3 peptide against MRSA was approximately $100\mu\text{M}$, while for blank G4 it was $80\mu\text{M}$ for all strains. However, when the strains were treated with the G4-QQ3 complex, the MIC₅₀ significantly decreased to $20\mu\text{M}$, and $15\mu\text{M}$, for MRSA, *S.aureus*, and *agr* mutants, respectively. This observation confirms that the potency of the peptide

increased after being loaded within the dendrimer and suggests a synergistic effect. All experiment performed as triplicate $p < 0.05$. Table 2 shows the MIC₅₀ for each nanoparticle.



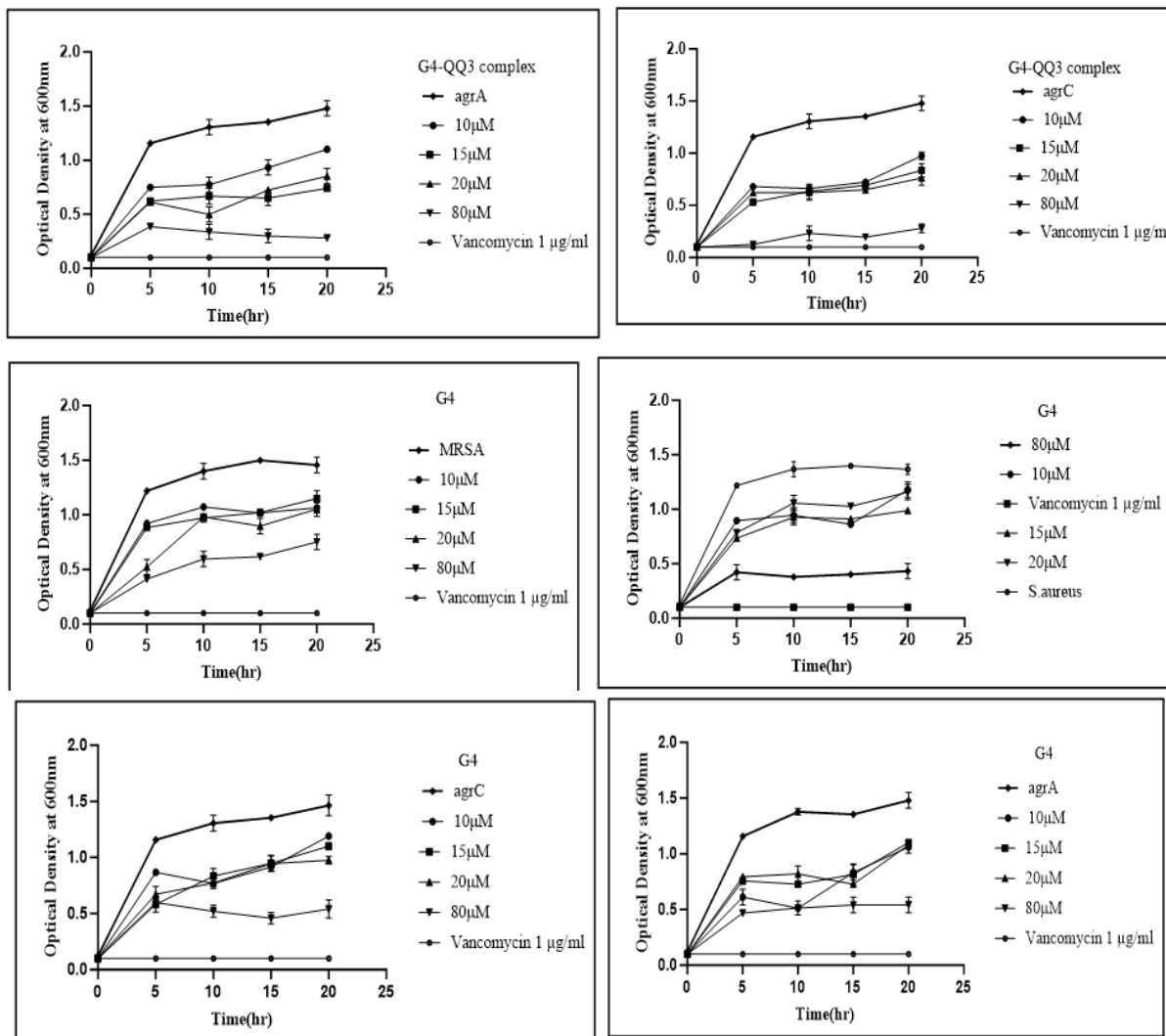


Figure 4. Growth curves of all strains. (mean \pm SD, n=3) ($p < 0.05$)

Nanoparticles	MRSA	<i>S.aureus</i>	<i>agrA</i> ,	<i>agrC</i>
G4-QQ3 complex MIC ₅₀ (μ M)	20	15	15	15
G4 MIC ₅₀ (μ M)	80	80	80	80
QQ3 MIC ₅₀ (μ M)	100	100	100	100

3.5 Biofilm inhibition assay:

After treating the cells with MIC₅₀% of the G4-QQ3 complex, it was able to inhibit the biofilm formation in all strains. The G4-QQ3 complex inhibit the biofilm in the MRSA, *S.aureus*, *agrA*, *agrC* by 65%, 71%, 69%, 86% respectively. While the blank G4 inhibit the biofilm in the MRSA, *S.aureus*, *agrA*, *agrC* by 48%, 31%, 49%, 50% respectively. The biofilm reduction by G4-QQ3 complex was significant ($p < 0.05$) as showed in figure 5.

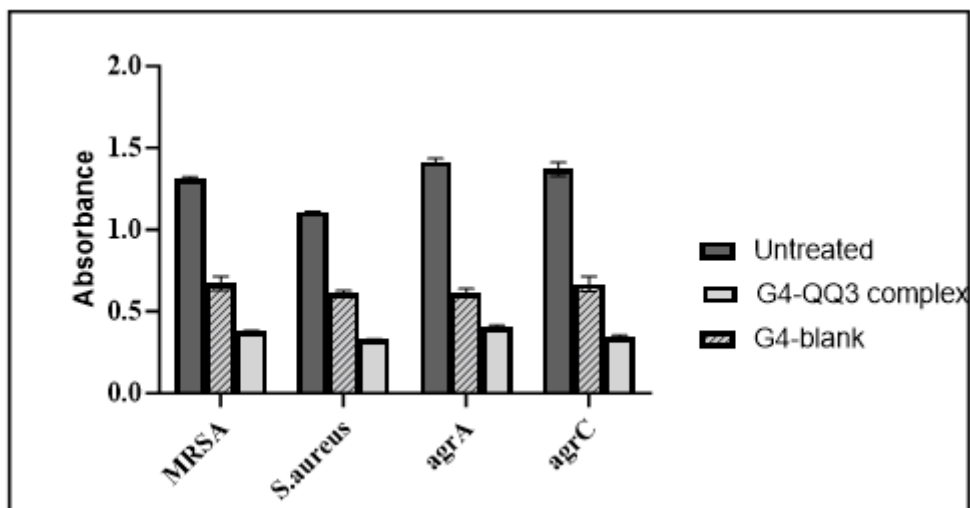


Figure 5. Inhibition of biofilm formation of MRSA, *S.aureus*, and *agr* mutants. (mean \pm SD, n=3) ($p < 0.01$).

3.6. Bacterial viability within formed biofilm after exposure to G4-QQ3 complex by confocal microscopic analysis. Live/dead stained for confocal laser scanning microscopy (CLSM) was used for all strains to determine the ability of the G4-QQ3 complex and blank G4 to kill the strains in the biofilm. Biofilm structure was visualized in the control untreated alive cells represented by green color. after treating the cells with MIC₅₀ of the loaded nanoparticles the number of dead bacterial cells were increase overtime after. Figure 6-9 shows the effect of loaded nanoparticles and blank G4 on all strains after 6(b) and 24(c) hr. This confirms the ability of the G4-QQ3 complex to kill the bacterial cells within the biofilm matrix.

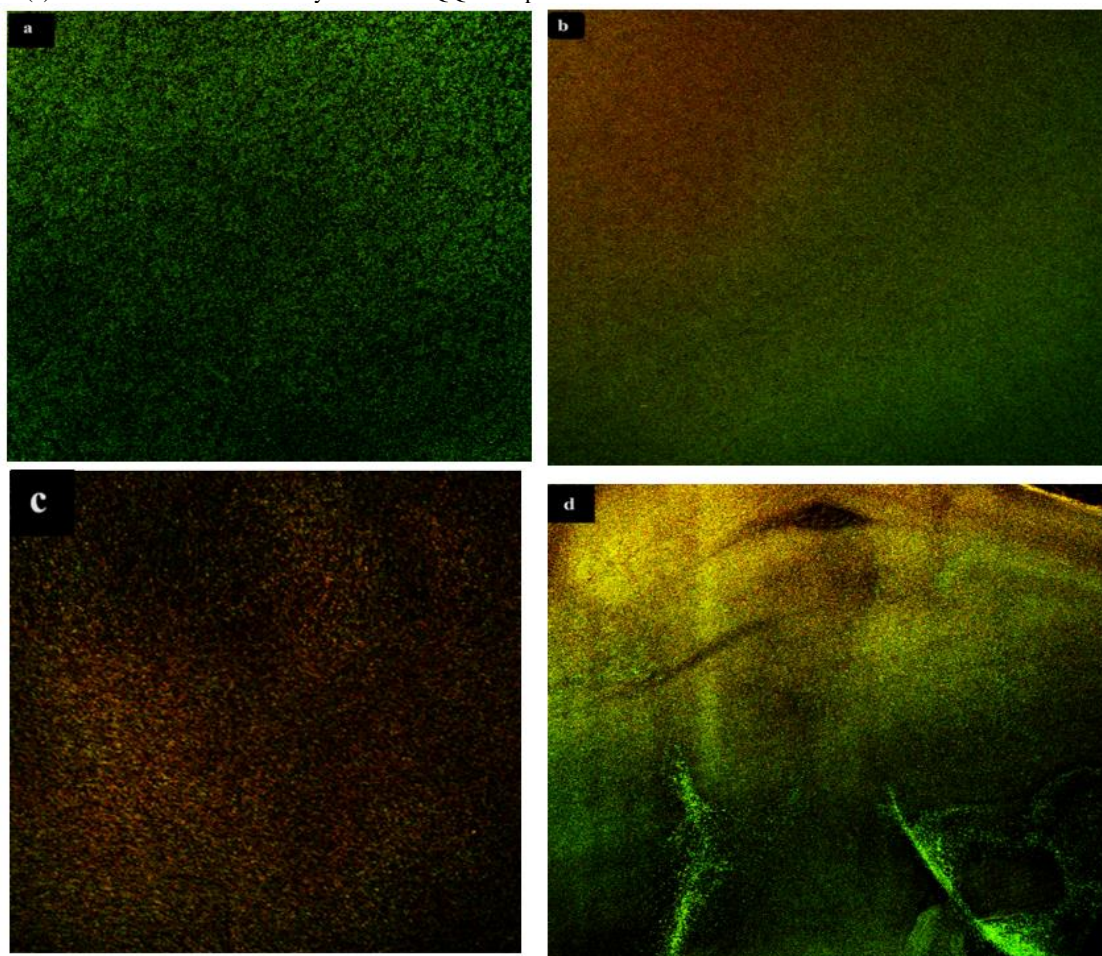


Figure 6. live/dead assay. The viability of MRSA after exposure to G4-QQ3 complex and blank G4. a) Control group in absence of loaded nanoparticles, b-c) MRSA treated with G4-QQ3 complex after 6h and 24h respectively, d) MRSA treated with blank G4. results showed a change in cell viability overtime, as an evidenced by the appearance of the red/yellow color that indicate dead cells.

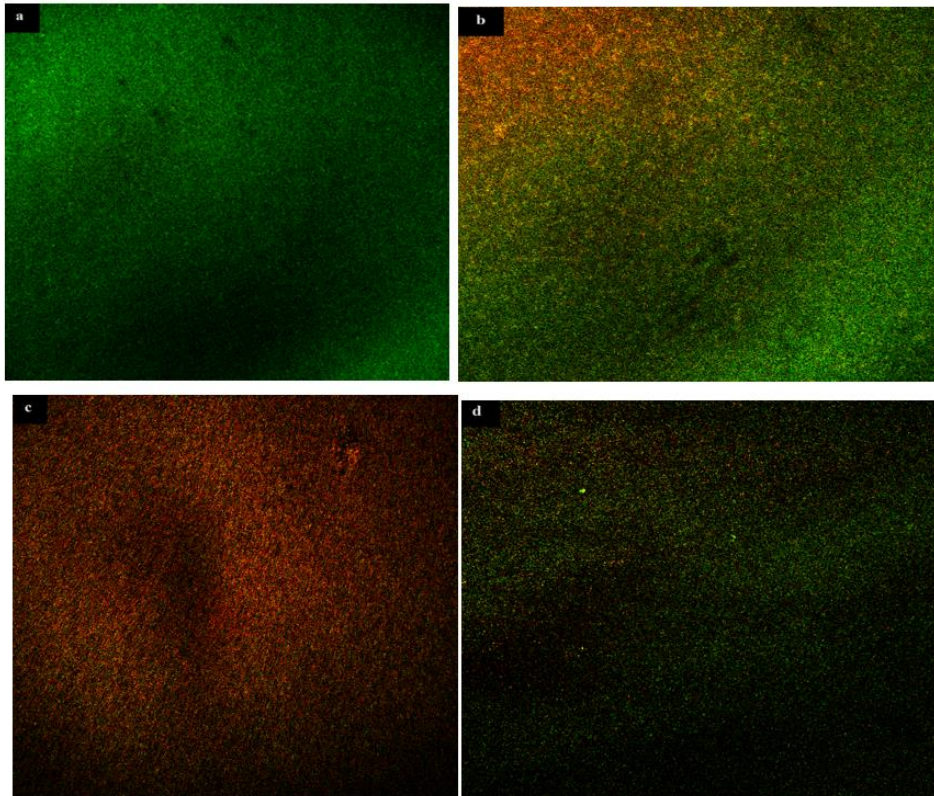


Figure 7. live/dead assay. The viability of *S.aureus* after exposure to G4-QQ3 complex and blank G4. a) Control group in absence of loaded nanoparticles, b-c) *S.aureus* treated with G4-QQ3 complex after 6h and 24h respectively, d) *S.aureus* treated with blank G4. results showed a change in cell viability overtime, as an evidenced by the appearance of the red/yellow color that indicate dead cells.

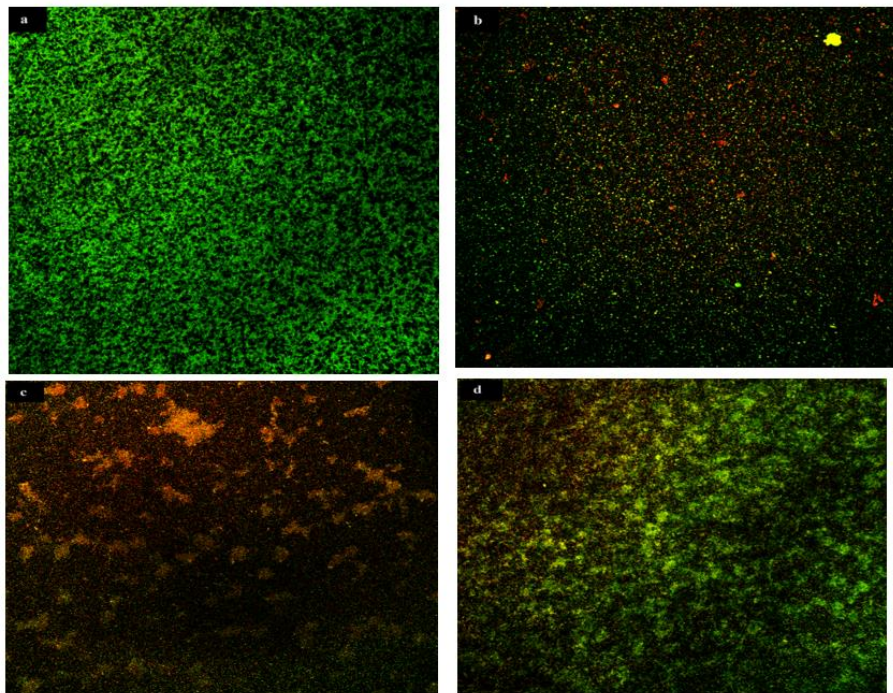


Figure 8. live/dead assay. The viability of *agrA* after exposure to G4-QQ3 complex and blank G4. a) Control group in absence of loaded nanoparticles, b-c) *agrA* treated with G4-QQ3 complex after 6h and 24h respectively, d) *agrA* treated with blank G4. results showed a change in cell viability overtime, as an evidenced by the appearance of the red/yellow color that indicate dead cells.

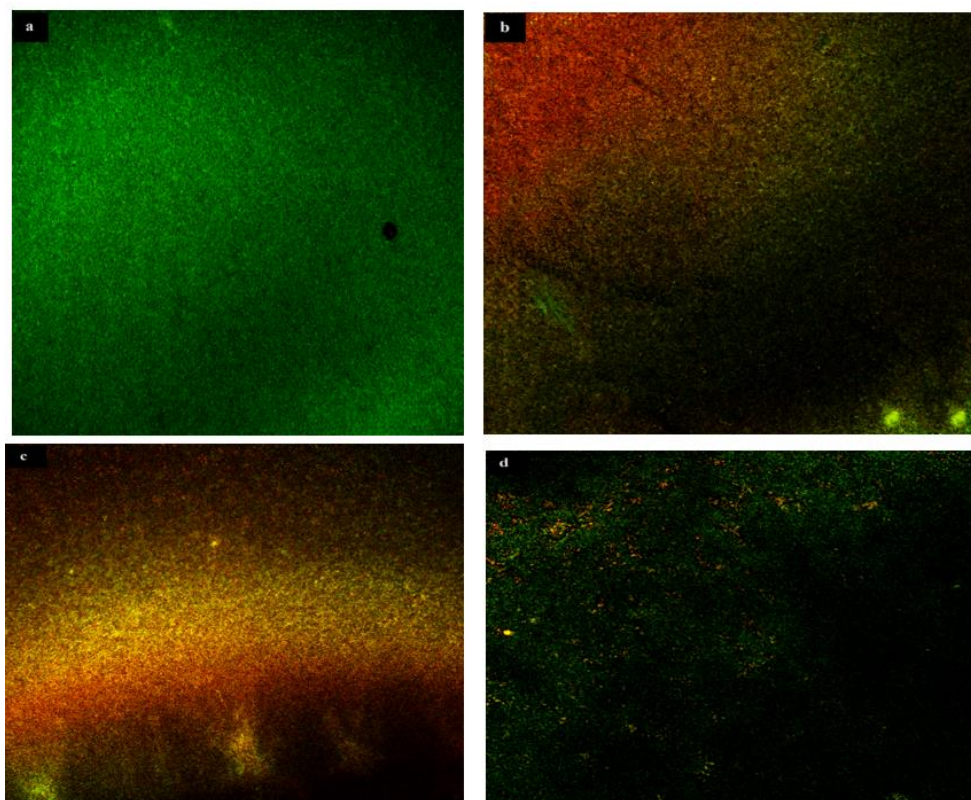
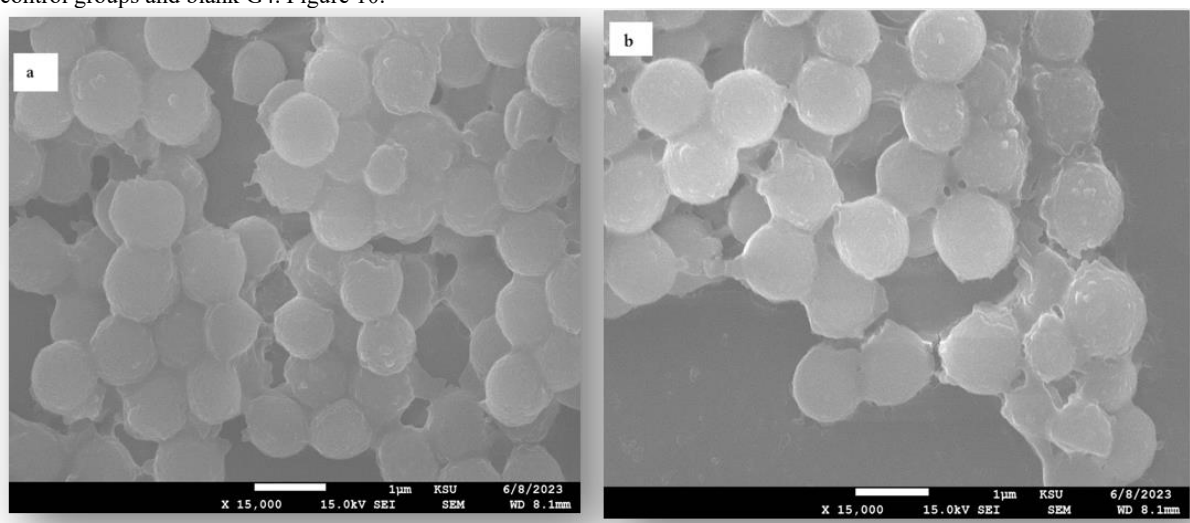
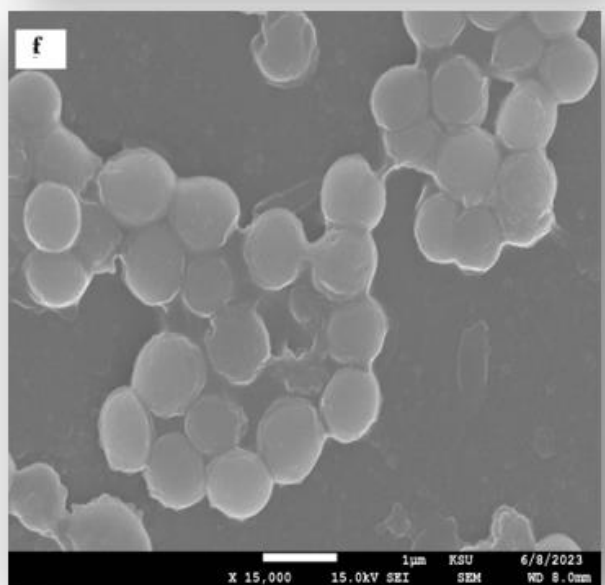
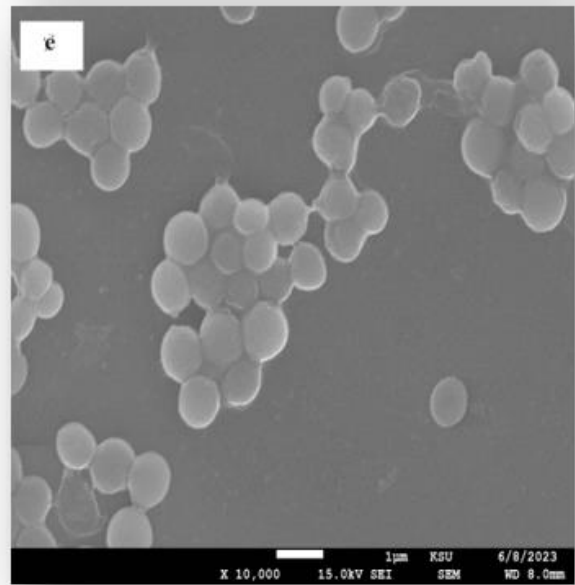
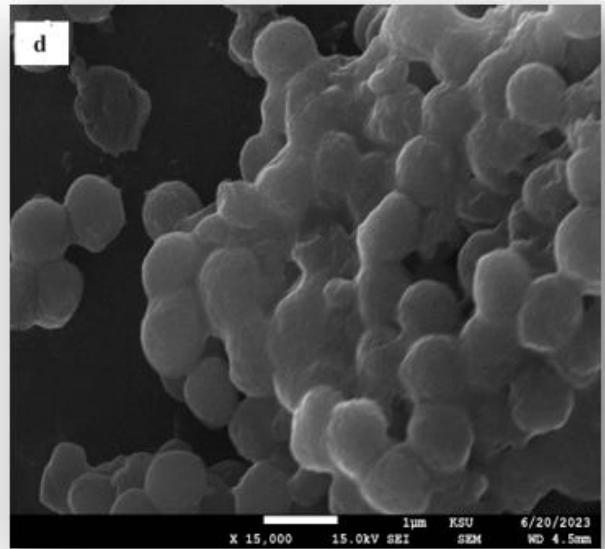
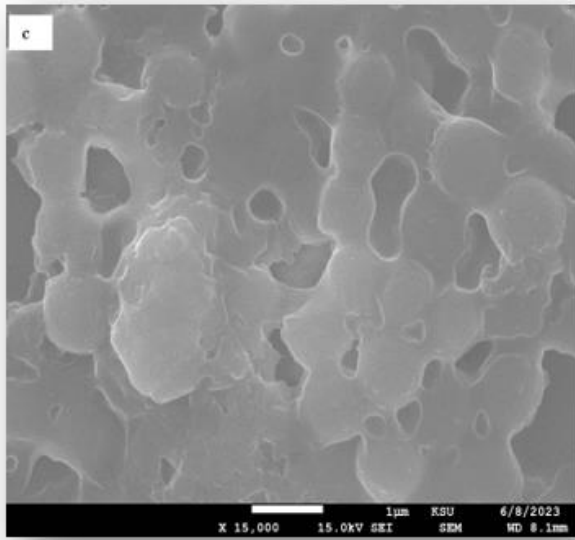


Figure 9. live/dead assay. The viability of *agrC* after exposure to G4-QQ3 complex and blank G4. a) Control group in absence of loaded nanoparticles, b-c) *agrC* treated with G4-QQ3 complex after 6h and 24h respectively, d) *agrC* treated with blank G4. results showed a change in cell viability overtime, as an evidenced by the appearance of the red/yellow colour that indicate dead cells.

3.7. SEM Images of G4-QQ3 complex and blank G4 treated bacterial biofilms:

All strains were visualized under SEM to investigate the morphology of the bacteria in the biofilms before and after treatment with the nanoparticles MIC₅₀. The findings from SEM images unambiguously demonstrate the presence of a substantial biofilm layer with a denser architecture enveloping the bacterial strain, which exhibits a greater propensity to form biofilms in *agr* mutant strains. Following exposure MIC₅₀ of each nanoparticle, the biofilm matrix exhibited a reduction in thickness and fragility, with a more pronounced eradication effect observed for the G4-QQ3 complex in comparison to the control groups and blank G4. Figure 10.





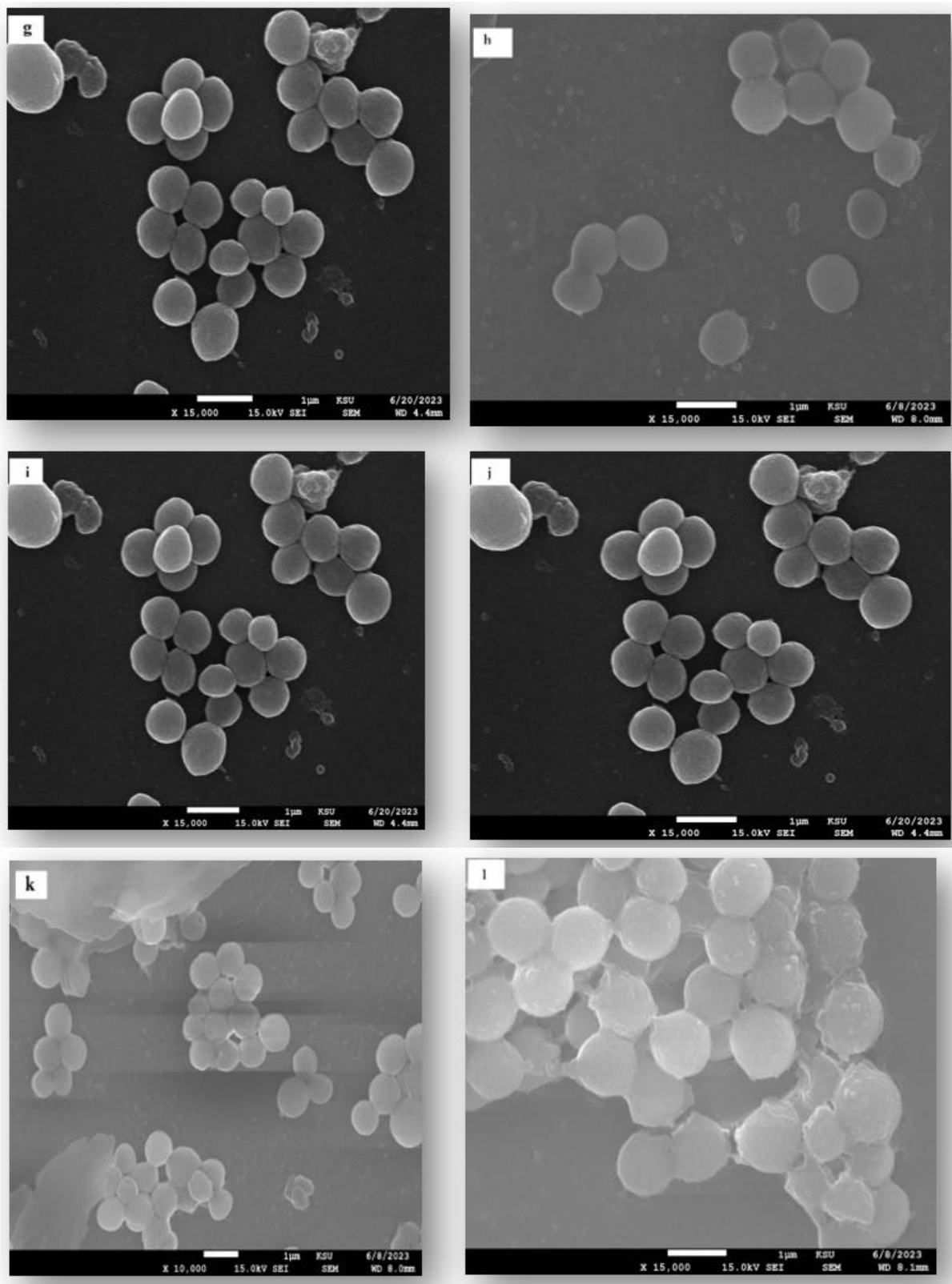


Figure 10. Scanning electron microscopy (SEM) images of a) Untreated MRSA, the biofilm is shown as dense extracellular matrix around the cells., b) Untreated *S.aureus*, c) Untreated *agrA* mutant, d) Untreated *AgrC* mutant. E, f, g, h) MRSA, *S.aureus*, *Agr A* mutant, and *Agr C* mutant treated with G4-QQ3 complex. I, j, k, l) MRSA, *S.aureus*, *Agr A* mutant, and *Agr C* mutant treated with blank G4.

3.8. Hemolysis assay:

The hemolysis activity of *S.aureus* and MRSA on blood agar was completely inhibited by the G4-QQ3 complex, as demonstrated in Figure 11, at concentrations of 3, 10, 15, and 20 μ M. Specifically, *S.aureus* hemolysis was completely inhibited at a concentration of 3 μ M, while MRSA required a higher concentration of 10 μ M for complete inhibition due to

its high resistance. In comparison, the blank G4 had limited effect on hemolysis when compared to the loaded nanoparticles. The hemolysis in *S.aureus* was inhibited by QQ3 at 10 μ M and this result is consistency with previous study [1] . while the MRSA treated with QQ3 peptide required a higher concentration up to 100 μ M to completely inhibit the hemolysis. This result confirms the anti-virulence activity of the formulated nanoparticles as it was able to inhibit a strong virulence activity of both strains with a low concentration.

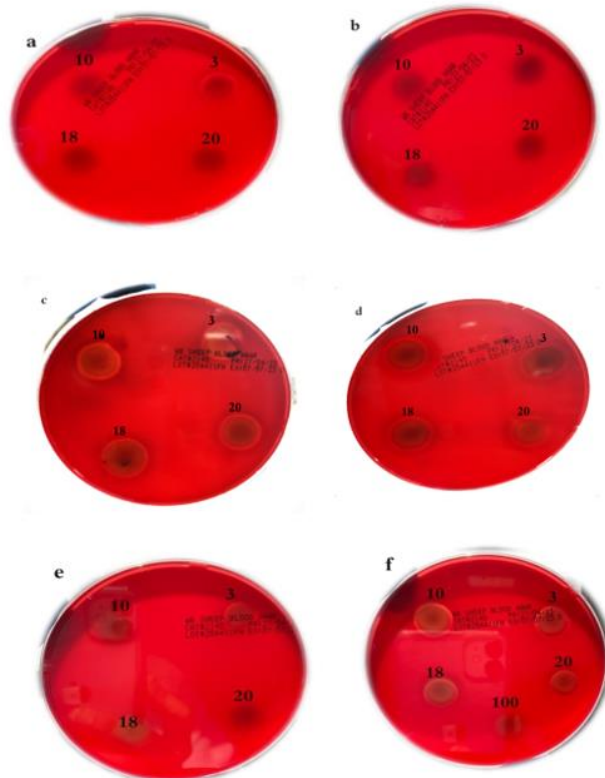


Figure 11. Hemolysis activity, a) MRSA treated with G4-QQ3 complex, at 3 μ M small zone of hemolysis are exist and it disappeared at 10 μ M b) *S.aureus* treated with G4-QQ3 complex, e) *S.aureus* treated with blank G5 naked QQ3, f) MRSA treated with QQ3 peptide hemolysis inhibited at 100 μ M.

3.9. In vitro Cytotoxicity

Different doses range 3 μ M to 40 μ M that include the MIC50% of the G4-QQ3 complex and blank G4 were used to assess their cytotoxicity against the very sensitive cell model RAW 264.7 cells. The result as shown in figure 12, confirm that G4-QQ3 complex and blank G4 were cytocompatible as the viability not significantly affected compared with control group.

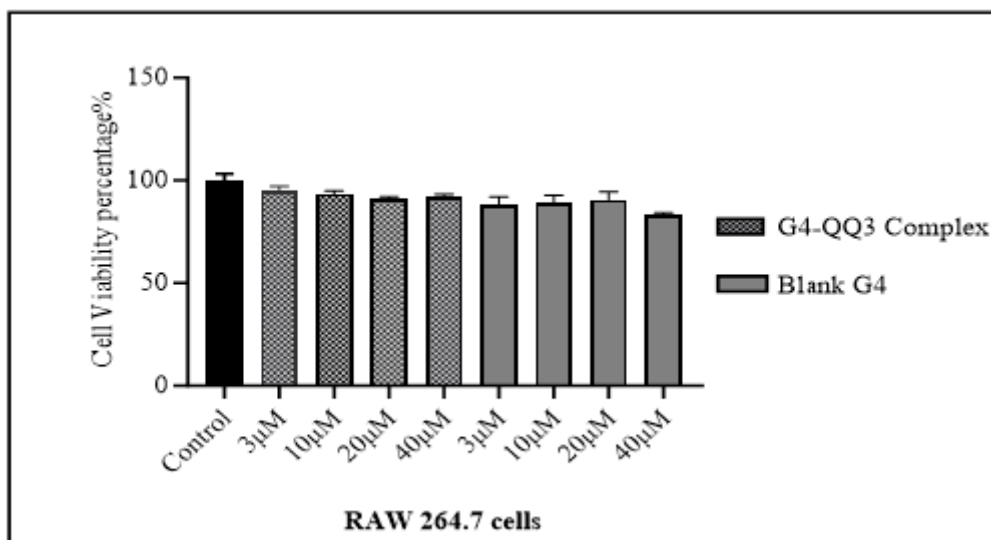


Figure 12. MTT assay for the G4-QQ3 complex and blank G4. (mean \pm SD, n=3)

DISCUSSION

MRSA is a predominant pathogen contributing to antimicrobial resistance (AMR) in both community and healthcare settings. Studies have shown that 33% of people carry *S.aureus* in their nose without harm, and two out of every hundred are MRSA carriers [14]. Quorum sensing (QS), is a mechanism that allows cell-to-cell communication due to the population expanding of the bacteria. In *S.aureus* quorum-sensing accessory gene regulator (*agr*) system controls the virulence factors production. In many diseases, the pathogenicity is multi-factorial, making it difficult to determine the precise role of each of these factors. Previous studies have found that mutation in the *agr* locus leads to a lack of expression of bacterial virulence factors. Targeting the QS with HK inhibitor will reduce the virulence in resistance strains such as *P. aeruginosa* [15]. A study identifies small molecules as HK inhibitors and tests them against MRSA. the result showed that these molecules can inhibit different HKs in vitro with antibacterial activity [11]. Recent studies found that cell-penetrating peptides (CPPs) and antimicrobial peptides (AMPs) have anti-microbial activity and can eradicate bacterial biofilm more efficiently compared to conventional antibiotics [16]. A previous study hypothesized that some of the quorum-quenching (QQ) peptides were able to reduce the amount of the AIP secretion in WT *S.aureus* compared with mutant *agrC*. The study concludes that QQ peptides work by altering the kinase activity by binding to *agrC* sensor domain and can inhibit the hemolysis activity in WT *S.aureus*[13].

Furthermore, QQ3 peptides used in this study are structurally different from the native AIP, and are larger macrocycles, having thioether linkage instead of thiolactone and no sequence similarity between them. This thioether group stabilizes the QQ3 peptides and prevents the post-translation modification that may occur. Different peptides having divergent primary structures have been tested on *S.aureus* and found that any alteration in the *agrC* ligand will inhibit the *agr* response. The inhibition may occur by noncovalent binding interaction that excludes the AIP from its receptor-binding pocket [14]. Antimicrobial peptides are emerging because of their bioactive property, target affinity, and high potency. The exact mechanism of action of this antimicrobial peptide is elusive and not fully understood. The suggested mechanism includes the peptide may induce complete or partial cell membrane lysis resulting in cell death, or it may cross the membrane and act on intracellular substances [15,16]. This study uses PAMAM G4 have carbomethoxy-pyrrolidone terminated. These dendrimers are water-soluble, biocompatible molecules with highly-branched structures that provide many surface areas that can be reactive to microorganisms. The biocompatibility and no immunogenicity are critical for using the dendritic structure. The cationic surface is commonly associated with toxicity. When modifying the surface with carbomethoxy- pyrrolidone moieties the PAMAM dendrimer acquired the biocompatibility features. This modification inhibits the activation of proinflammatory human monocytes with reduced toxicity [17]. Also, studies use the PAMAM dendrimers to encapsulate silver and it showed a strong antimicrobial activity against gram-positive organisms. PAMAM biocidal activity against *S.aureus*, contributed to membrane destruction, and the release of cytoplasmic contents was observed [18,19].

The particles' morphology was determined using TEM. The nanoparticles for G4-QQ3 complex, and blank G4 were observed to have an almost spherical shape especially in the blank nanoparticles, and a size of approximately 283 nm for the loaded nanoparticles and blank G4 was less than 200nm. The difference in size between the blank and loaded nanoparticles proves that the loading of the drug was successful. The zeta potential for blank G4 was -1.3 mV. The negative charge was increased upon loading the peptide which has a negative charge to reach -19 mV for the G4-QQ3 complex. The present study has revealed that the liberation of the peptide from the G4-QQ3 takes place in a continuous and protracted manner, spanning a period of approximately 72 hours. The overall release percentage was determined to be 80%, while the encapsulation efficiency was found to be 98%.

Moreover, one of the most potent virulence factors that MRSA use is the secretion of toxins (α , β , γ , δ) which facilitate spreading, cause tissue damage, nutrient uptake, and makes pores in the membrane, leading to the efflux of essential molecules and metabolites. Reducing or inhibiting these hemolysins will reduce the severity of infection and delay the development of biofilms.

The hemolytic activity of the *S.aureus*, and MRSA was tested. In a previous study [13] the hemolysis activity of *S.aureus* was inhibited with QQ3 peptide at a concentration of 10 μ M and the effect of QQ3 on MRSA has never been tested. In this study, the QQ3 peptide was able to inhibit the hemolytic activity of MRSA at a concentration of 100 μ M. When loading the peptide on PAMAM G4 dendrimer the inhibitory concentration was reduced for both *S.aureus* and MRSA to 3 μ M and 10 μ M respectively. Blank G4 limited the hemolysis activity but did not inhibit it completely compared with loaded nanoparticles. The bacterial growth curve of all strains showed that G4-QQ3 complex inhibits the bacterial growth of *S.aureus* wild type, MRSA, *agrA* mutant, and *agrC* mutant at MIC50% 20 μ M. Whereas, blank G4 only reduces the rate of growth at 80 μ M. MRSA treated with naked QQ3 peptide showed an inhibition of growth with a high concentration of 100 μ M. This result confirms that PAMAM G4 dendrimer is important for encapsulating the peptide and preventing its uptake by the bacterial cells, and suggesting a synergism effect. When treating MRSA with G4-QQ3 complex a lower concentration (20 μ M) was required to inhibit the growth of the strain, compared with 100 μ M and 80 μ M for the QQ3 peptide and G4 blank respectively. By blocking hemolysin expression, and inhibiting bacterial growth in all strains, these results confirm the potent anti-virulence and antimicrobial properties of nanoparticles complex and suggest a synergism effect.

The biofilm formation is one of the most potent virulence factors that *S.aureus*, and MRSA phenotype use to resist antibiotics. In prosthetic implants, *agr* mutants are frequently isolated. Bacteria within biofilms can be up to 1,000 times more resistant to antibiotics than plank- tonic cells [4]. The *agr* system regulates the switch between planktonic and biofilm lifestyles and has a crucial role in biofilm development. Findings from antibiofilm assay, SEM image, and live\dead viability

assay, all together confirm that G4-QQ3 complex was able to inhibit, penetrate, and eradicate the biofilm and, kill all strains within the biofilm structure. The percentage of biofilm inhibition for G4-QQ3 complex ranged from 65 to 71%, while for the blank G4 the percentage was lower ranged 31% to 50%. Examine the morphology of bacterial cell within biofilm by SEM illustrate that nanoparticles were able to eradicate the biofilm matrix. Live\dead viability assay confirm the potency of the formula as it was able to kill the bacteria within biofilm structure as represented by the red\yellow colour under confocal microscope. These results prove the potent antibacterial and anti-virulence actions of the formulated nanoparticles. Also, this suggests that G4-QQ3 complex not only works as an inhibitor for *agrC*, as it inhibits the biofilm formation and growth of the *agrC* mutant strain, it may target another component in the *agr* system, or disrupt cell membrane. As noted earlier the phosphorylation of *agrA* is catalyzed by *AgrC* and both form the TCS, using inhibitors for *agrC* or *agrA* will be efficient antagonists of the *agr* system. Some *S.aureus* strains I311T and F264C acquire *agrC* mutation naturally and these were associated with delayed and reduced AIP production without abolishing the activity. Also, induced point mutation in *agrC* in ST22 and ST239 are *S.aureus* strains that cause a delay in AIP production, but it responded to exogenous AIP. Thus, the *agr* system is complex and controlled by numerous regulators, inhibitors, and other factors protein. The activity of these alternative factors may be responsible for the sensitivity to the exogenous *agrC* ligand, but the underlying mechanism is not clear [20]. Also, it was reported that using AIPs from other staphylococcal species can downregulate the function of the *agr* system. Some peptides that have a district structure from native AIP may act as an allosteric inhibitor of *AgrC* [21].

An ideal antimicrobial agent should be non-toxic to host cells and toxic to microbial cells. RAW 264.7 cells were used to investigate the cytotoxicity effect of the formulated nanoparticles. This cell line is an appropriate model of macrophages and is considered a very sensitive cell line. MRSA can survive within the phagocytes and this intracellular stage is crucial for persistence, dissemination, and infection [22]. The G4-QQ3 complex and blank G4 were tested against RAW 264.7 cells and the result showed that the G4-QQ3 complex and blank G4 are cytocompatible to concentrations up to 40 μ M.

In this study, PAMAM G4 loaded with HK inhibitor peptide QQ3 results in antimicrobial action against a highly resistance strain MRSA, and against *S.aureus* WT and QS mutant. The QQ3 peptide was encapsulated by the PAMAM G4, this protects the peptide to exert its action by either competitive binding to the sensor HK *agrC*, thus preventing AIP-*agrC* interaction and disrupting the *agr* system. Other proposed mechanism includes; targeting other intercellular component or disrupting cell membrane. Both actions led to inhibiting important virulence factor production in *S.aureus* and MRSA phenotype [23,24]. Furthermore, the study suggests that PAMAM G4 and QQ3 produce a synergistic effect as both have antimicrobial action that was evaluated with different in-vitro methods on different strains; MRSA, *S. au-reus*, and QS mutant. The synergistic effects of this complex were examined on planktonic bacterial cells, and their efficacy on biofilm inhibition was tested. The formulated nanoparticles showed a cytocompatible feature when tested against RAW 264.7 cells. Anti-virulence drug development are attractive target and the chance of resistance to this therapy is low as the antimicrobial does not threaten the survival of the microbe.

CONCLUSIONS

The emergence of antimicrobial resistance among pathogenic bacteria, including Methicillin-resistant *Staphylococcus aureus* (MRSA), poses a significant threat to public health. Novel strategies are required to combat this issue, and one such approach is the use of quorum sensing inhibitors. In this study, the G4-QQ3 complex were synthesized, and they exhibited a minimum particle size, maximum encapsulation efficiency, and sustained in vitro release. These nanoparticles demonstrated potent antibacterial and anti-virulence activity against all tested *S.aureus* and MRSA phenotypes, effectively reducing, penetrating, and eradicating biofilm formation. The results of this study suggest that G4-QQ3 complex hold potential for future therapeutic use in the treatment of MRSA and *S.aureus* infections, as well as in the prevention of biofilm formation. Ongoing efforts should be directed towards identifying new targets that can limit bacterial growth or reduce the severity of infection.

Author Contributions: FSA, FYA and NAA: Conceptualization, design of study, methodology, acquisition of data, validation, supervision Resources, visualization and writing final draft preparation. NAA: Acquisition of data, analysis of data, visualization, interpretation of data and writing final draft preparation. AAA and MMA: cytotoxicity study, investigation, interpretation of all chemical analysis, and validation. RTA interpretation of data and chemical analysis of nanoparticles. All authors have read and agreed to the published version of the manuscript.

Funding: Deanship of scientific research in King Saud University for funding and supporting this research through the initiative of DSR Graduate Students Research Support (GSR). King Saud University, Riyadh, Saudi Arabia.

Institutional Review Board Statement: Not applicable.

Informed Consent Statement: Not applicable.

Data Availability Statement: The data presented in this study are available on request from the corresponding author.

Acknowledgments: The authors would like to thank Deanship of scientific research in King Saud University for funding and supporting this research through the initiative of DSR Graduate Students Research Support (GSR), King Saud University, Riyadh, Saudi Arabia.

Conflicts of Interest: The authors declare no conflict of interest.

REFERENCES:

1. Aljeldah, Mohammed,. Prevalence of Methicillin-Resistant Staphylococcus aureus (MRSA) in Saudi Arabia: A Systematic Review.. *J Pure Appl Microbiol.* 2020;46.(46.).
2. Al Bshabshe, A., Joseph, M., Awad El-Gied, A., Fadul, A., Chandramoorthy, H. and Hamid M. Clinical Relevance and Antimicrobial Profiling of Methicillin-Resistant Staphylococcus aureus (MRSA) on Routine Antibiotics and Ethanol Extract of Mango Kernel. *Biomed Res Int.* Published online 2020:1-8.
3. Grundstad, M., Parlet, C., Kwiecinski, J., Kavanaugh, J., Crosby, H., Cho, Y., Heilmann, K., Diekema, D. and Horswill A. Quorum Sensing, Virulence, and Antibiotic Resistance of USA100 Methicillin-Resistant Staphylococcus aureus Isolates. *mSphere.* 2019;4(4).
4. Yarwood J. M., Schlievert P. M. Quorum sensing in Staphylococcus infections. *J. Clin. Invest.* (2003). 112 1620–1625. 10.1172/JCI20442
5. Nielsen, A., Månsson, M., Bojer, M., Gram, L., Larsen, T., Novick, R., Frees, D., Frøkiær, H. and Ingmer H. Solonamide B Inhibits Quorum Sensing and Reduces Staphylococcus aureus Mediated Killing of Human Neutrophils. *PLoS ONE.* 2014;9(1),.
6. Choudhary KS, Mih N, Monk J, Kavvas E, Yurkovich JT, Sakoulas G PB. The Staphylococcus aureus Two-Component System AgrAC Displays Four Distinct Genomic Arrangements That Delineate Genomic Virulence Factor Signatures. *Front Microbiol.* 2018;25:9:(1082).
7. Prieto, J.M., Rapún-Araiz, B., Gil C et al. Inhibiting the two-component system GraXRS with verteporfin to combat Staphylococcus aureus infections. *Sci Rep.* 2020;10,(17939).
8. Zhou Y, Huang L, Ji S, Hou S, Luo L, Li C, Liu M, Liu Y JL. Structural basis for the inhibition of the autophosphorylation activity of HK853 by luteolin. *Mol 2.* 2019;24:933.
9. Velikova, N., Fulle, S., Manso A et al. Putative histidine kinase inhibitors with antibacterial effect against multi-drug resistant clinical isolates identified by in vitro and in silico screens. *Sci Rep.* 2016;6, 26085.
10. de Alteriis E, Lombardi L, Falanga A, Napolano M, Galdiero S, Siciliano A, Carotenuto R, Guida M GE. Polymicrobial antibiofilm activity of the membranotropic peptide gH625 and its analogue. *Microb Pathog.* 2018;125(189-195).
11. Tiwari S, Jamal SB, Hassan SS, et al. Two-component signal transduction systems of pathogenic bacteria as targets for antimicrobial therapy: An overview. *Front Microbiol.* 2017;8(OCT).
12. Janaszewska A, Lazniewska J, Trzepiński P, Marcinkowska M, Klajnert-Maculewicz B. Cytotoxicity of dendrimers. *Biomolecules.* 2019;9(8):1-23.
13. Xie Q, Wiedmann MM, Zhao A, et al. Discovery of quorum quenchers targeting the membrane-embedded sensor domain of the Staphylococcus aureus receptor histidine kinase, AgrC. *Chem Commun.* 2020;56(76):11223-11226.
14. 14.CDC. (2019). Healthcare Settings | MRSA | CDC. *Cdc.gov.* [online]. Available from: <https://www.cdc.gov/mrsa/healthcare/index.html>.
15. Fihn CA, Carlson EE. Targeting a highly conserved domain in bacterial histidine kinases to generate inhibitors with broad spectrum activity. *Curr Opin Microbiol.* 2021;61:107-114. doi:10.1016/j.mib.2021.03.007
16. Ma, L., Xie, X., Liu, H., Huang, Y., Wu, H., Jiang, M., Xu, P., Ye, X., Zhou, C. (2020). Potent antibacterial activity of MSI-1 derived from the magainin 2 peptide against drug-resistant bacteria. *Theranostics*, 10(3), 1373-1390. <https://doi.org/10.7150/thno.39157>.
17. Velikova, N., Fulle, S., Manso A et al. Putative histidine kinase inhibitors with antibacterial effect against multi-drug resistant clinical isolates identified by in vitro and in silico screens. *Sci Rep.* 2016;6, 26085.
18. de Alteriis E, Lombardi L, Falanga A, Napolano M, Galdiero S, Siciliano A, Carotenuto R, Guida M GE. Polymicrobial antibiofilm activity of the membranotropic peptide gH625 and its analogue. *Microb Pathog.* 2018;125(189-195).
19. Falanga A, Del Genio V GS. Peptides and Dendrimers: How to Combat Viral and Bacterial Infections. *Pharm .* 2021;13(1):101.
20. Studzian M, Działak P, Pułaski Ł, Hedstrand DM, Tomalia DA, Klajnert-Maculewicz B. Synthesis, Internalization and Visualization of N-(4-Carbomethoxy) Pyrrolidone Terminated PAMAM [G5:G3-TREN] Tecto(dendrimers) in Mammalian Cells. *Molecules.* 2020 Sep 25;25(19):4406. doi: 10.3390/molecules25194406.
21. Fihn CA, Carlson EE. Targeting a highly conserved domain in bacterial histidine kinases to generate inhibitors with broad spectrum activity. *Curr Opin Microbiol.* 2021;61:107-114. doi:10.1016/j.mib.2021.03.007
22. Sloan TJ, Murray E, Yokoyama M, Massey RC, Chan WC, Bonev BB, Williams P. Timing Is Everything: Impact of Naturally Occurring *Staphylococcus aureus* AgrC Cytoplasmic Domain Adaptive Mutations on Autoinduction. *J Bacteriol.* 2019 Sep 20;201(20):e00409-19. doi: 10.1128/JB.00409-19. PMID: 31358609; PMCID: PMC6755735.
23. English BK, Maryniw EM, Talati AJ, Meals EA. Diminished macrophage inflammatory response to Staphylococcus aureus isolates exposed to daptomycin versus vancomycin or oxacillin. *Antimicrob Agents Chemother.* 2006;50(6):2225-2227. doi:10.1128/AAC.01559-05
24. N. Malik, R. Wiwattanapatapee, R. Klopsch, K. Lorenz, H. Frey, J. W. Weener, E. W. Meijer, W. Paulus and R. Duncan J. *Handbook of Nanobiomedical Research: Fundamentals, Applications.* Vol 3. (Torchilin V, ed.); 2014.
25. Sharma D, Misra L, Khan AU. Antibiotics versus biofilm: an emerging battleground in microbial communities. *Antimicrob Resist Infect Control.* 2019 May 16;8:76. doi: 10.1186/s13756-019-0533-3. PMID: 31131107; PMCID: PMC6524306.